Highly Efficient Asymmetric Paternò–Büchi Reaction in a Microcapillary Reactor Utilizing Slug Flow

Kimitada Terao, Yasuhiro Nishiyama and Kiyomi Kakiuchi*

Graduate School of Materials Science, Nara Institute of Science and Technology (NAIST), 8916-5 Takayama-cho, Ikoma, Nara 630-0192, Japan

Received: 4 December 2013; accepted: 29 December 2013

An asymmetric Paternò–Büchi-type photoreaction between 2,3-dimethyl-2-butene and benzoylformic acid ester with a chiral menthyl auxiliary was studied in a continuous-flow microcapillary reactor. The fluorinated ethylene propylene (FEP) microcapillary reactor using normal one-layer flow mode gave oxetane products with better efficiency than the batch system. In addition, the slug flow mode in microcapillary reactor using inactive reagent, N_2 gas or H_2O, improved the reaction efficiency dramatically because of synergistic light dispersion, stirring and thin layer film effects. The reaction efficiencies under each condition were discussed as energy efficiencies calculated from reactors' parameters.

Keywords: photochemistry, flow reactor, slug flow mode, Paternò–Büchi photoreaction, asymmetric reaction

1. Introduction

Photochemical reactions using photons as sustainable reagents enable the formation of complex structures that cannot be obtained easily using thermal reactions [1]. In spite of this potential, however, photoreactions are rarely adopted for use on an industrial scale. One of the main reasons for this is the low light irradiation efficiency of traditional batch reactors, which is caused by attenuation based on the Lambert–Beer law, $A=\varepsilon \times c \times l$ (A, absorbance; ε, absorption coefficient; c, molar concentration; l, path length). On the other hand, microflow reactors [2], which are devices with micrometer-sized inner dimensions, have recently shown promise for improving the efficiency of photoreactions owing to the large surface and irradiation areas [3]. A number of processes have been published that utilize this methodology, for example, the Pauson–Khand reaction [4a], oxidation reactions [4b], [2+2] addition reactions [4c], the synthesis of vitamin D3 [4d] and artemisinin [4e], among others [5]. Although interest in the use of microreactor techniques for photoreactions has increased, asymmetric processes have not been widely discussed [6]. Within this field, our group has previously reported diastereoselective [2+2] photoadditions of cyclopentene to cyclohexenones with chiral menthyl auxiliaries using a photo-microreactor [7]. Compared to batch processes, higher selectivity and productivity were achieved under these microflow conditions. In addition, heterogeneous [2+2] photoreactions using ethylene gas as a reagent in a microcapillary reactor was also reported, with high energy efficiency enabled by the two layers of ethylene gas and substrate solution that were formed [8]. Oelgemöller's group has also reported on the efficiency of photoreactions using slug flow involving a gaseous reagent and a solution [9]. From these reports, we envisaged that slug flow utilizing an inactive gas or inactive liquid in combination with the reaction solution in a microcapillary reactor may improve the efficiency of photoreactions. To verify this hypothesis, we chose an asymmetric Paternò–Büchi-type photoreaction of 2,3-dimethyl-2-butene **2** to benzoylformic acid ester **1** [10], containing a chiral menthyl auxiliary (Scheme 1) as a model reaction, and examined it in both batch and microcapillary mode. The Paternò–Büchi-type photoreaction is a typical [2+2] photoaddition of an alkene to a carbonyl compound, giving an oxetane structure in a single step and is potentially applicable to the synthesis of many bioactive compounds [11].

Scheme 1. The employed Paternò–Büchi reaction

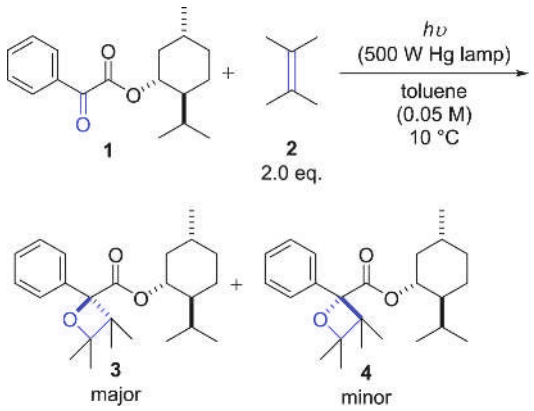

Herein, we describe a highly efficient asymmetric Paternò–Büchi reaction carried out in a microcapillary reactor using slug flow.

2. Results and Discussion

The reaction setup is shown in Figure 1. Teflon, fluorinated ethylene propylene copolymer (FEP; $\lambda > 230$ nm), was employed as the microcapillary reactor (inner diameter; i.d.: 1.0 mm). The flexible tube was tightly wrapped around a quartz immersion well (outer diameter; o.d.: 17.5 cm) with a common high-pressure Hg lamp (500 W) at its center. The entire setup was submerged in a MeOH-containing cooling bath set at 10 °C. This was then covered with aluminium foil, along with the light source and irradiation unit, in order to increase the light intensity by reflecting the UV light [12]. Three different flow conditions were established within the reactor: 1. normal flow mode, 2. slug flow mode with N_2 gas, and 3. slug flow mode with water. The asymmetric Paternò–Büchi-type photoreaction between **1** and **2** was also examined in a conventional batch type reactor consisting of a Pyrex test tube (i.d.: 14 mm; $\lambda > 280$ nm) as the reaction vessel. Conversion of substrate **1** was determined using ^{1}H NMR analysis, and the yields and diastereomeric excess (d.e.) values were determined using gas chromatography (GC) analysis of the crude reaction mixture.

For all flow conditions, the yields of target compounds **3** and **4** increased with extended irradiation time, however, the d.e. value remained relatively constant. In the batch reactor (Table 1, entries 1–4), 420 sec irradiation gave 100% conversion of substrate **1** in 54% yield (entry 4). On the other hand, under

* Author for correspondence: kakiuchi@ms.naist.jp

DOI: 10.1556/JFC-D-13-00035

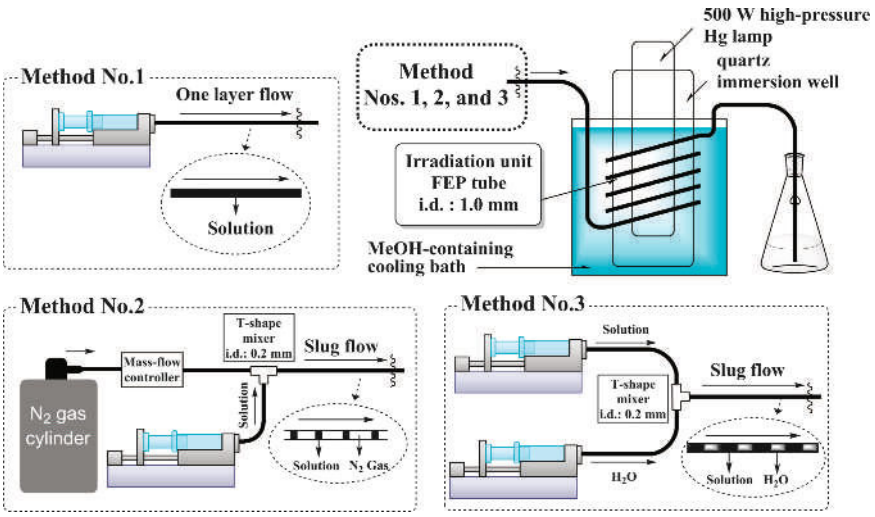

Figure 1. Flow-modes in the FEP microcapillary reactor

Table 1. Flow-mode effects on Paternò–Büchi-type reaction

Entry	Method	Solution flow rate (mL min^{-1})	N_2 or H_2O flow rate (mL min^{-1})	Irr. time (sec)	Yield[a] (%)	Conversion[b] (%)	d.e.[a] (%)
1	batch			60	19		51
2				180	40		51
3				300	53		51
4				420	54	100	50
5	No.1	3.142		15	31		50
6		1.571		30	39		52
7		0.7854		60	53	100	50
8	No.2	0.25	5.0	32	36		50
9		0.25	3.0	44	44		50
10[c]		0.25	5.0	32	55	100	49
11[c]		0.25	3.0	44	56	100	50
12	No.3	3.142	3.142	7.5	24		50
13		1.571	1.571	15	45		49
14		0.7854	0.7854	30	56	100	51

[a] Determined by by GC analysis using *n*-tetracosane as an internal standard. [b] Determined by ^{1}H NMR. [c] Other trials.

normal flow conditions in the microcapillary reactor (method 1, entries 5–7), the substrate was completely consumed after only 60 sec irradiation, and the yield of 53% was maintained (entry 7). Under the slug flow conditions, using the reaction solution and N_2 gas (method 2, entries 8, 9), 44% yield was achieved after 44 sec irradiation, but a proportion of substrate **1** still remained, and the yield was lower than that obtained under normal flow conditions (entry 9). However, these results were not reproducible, with other trials (entries 10, 11), demonstrating complete consumption of **1** in only 32 sec. We concluded that the slug flow conditions of method 2 were hard to control because of the solubility of N_2 gas in the reaction solution and/or back pressure. We therefore altered the conditions to obtain slug flow using H_2O and substrate solution (method 3, entries 12–14). This flow mode was found to be easier to control than that using N_2, and a yield of 56% and 100% conversion were achieved in only 30 sec (entry 14 vs. 6). We confirmed the absence of substrate **1**, and products **3** and **4** in the H_2O layer after photoirradiation. These results indicate that the microcapillary conditions generally accelerated the photoreaction, and the slug flow conditions using H_2O further improved the yield. On the other hand, the diastereoselectivities did not change under any conditions.

The effect of flow rate ratio under slug flow conditions using H_2O was examined after 15 sec photoirradiation (Table 2). The ratio of flow rates (solution flow rate/H_2O flow rate) was varied from 0.25 to 4.0, and the length of reaction solution segments in the capillary were extended as the flow rate ratio was increased. As a result, at ratios of 2.0–4.0, almost the same yield was achieved as that under normal flow conditions (entries 2, 3 vs. 1). On the other hand, at ratios of 0.25–1.0, higher yields were obtained (entries 4–6 vs. 1), with the lowest ratio giving the highest yield. This demonstrated that better yields could be achieved by using a lower substrate solution flow rate.

To account for the superior performance of the microcapillary reactor, the UV transmission of substrate **1** at 365 nm was calculated from its absorption spectrum in toluene using the Lambert–Beer law (Figure 2). The transmission through the capillary of the microflow reactor was determined to be 63%, while that of the Pyrex test tube was close to 0%. From the difference in transmission between the two materials, it was deduced that the light more effectively irradiated the reaction solution in the microcapillary reactor. In addition, the confinement effect of light derived from the difference of refractive index may also contribute to this unique result. When light passes through a medium with a large refractive index into one with a lower index, all light is reflected by the former, which is termed total reflection. The refractive index of FEP is 1.34 [13], while that of toluene is higher at 1.50 [14], indicating

Table 2. Effects of flow rate ratios after 15 sec irradiation

Entry	Solution flow rate (mL min^{-1})	H_2O flow rate (mL min^{-1})	Ratio (solution/H_2O)	Yield[a] (%)	de[a] (%)
1	3.142			31	50
2	2.513	0.6283	4.0	33	50
3	2.095	1.047	2.0	36	48
4	1.571	1.571	1.0	45	49
5	1.047	2.095	0.50	52	50
6	0.6283	2.513	0.25	55	51

[a] Determined by GC analysis, using *n*-tetraconsane as an internal standard.

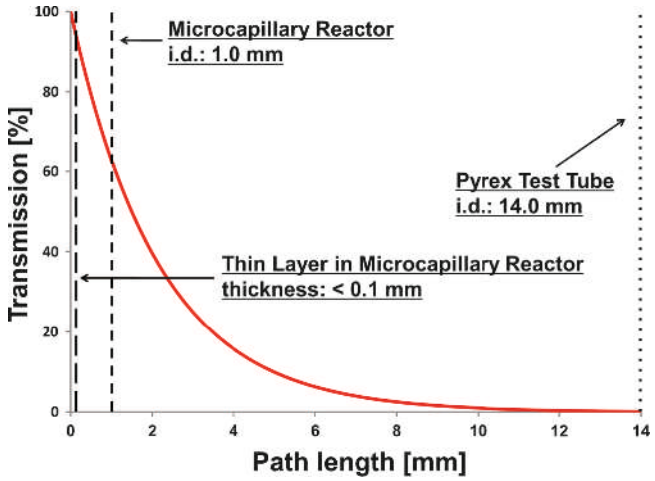

Figure 2. Light transmission of **1** in toluene at 365 nm

the feasibility of total reflection occurring in the reaction solution within the FEP tube, similar to the case of optical fibers. As a result, the light could have been repeatedly reflected, thereby accelerating the photoreaction in the microcapillary reactor.

The high performance achieved using the slug flow mode involving the substrate solution and H_2O was speculated to depend on three factors (Figure 3). The first of these is a light dispersion effect, whereby the irradiated light is dispersed by the FEP capillary wall, causing the reaction solution to be irradiated from multiple directions, accelerating the reaction. This effect may be seen more clearly with small segments and when only short irradiation times are necessary for achieving the reaction. The second contributing factor is stirring caused by movement of the H_2O, as has been previously reported for microdevices [15].

Our group has previously reported that slug flow conditions using a reagent gas and reaction solution in a microcapillary created a very thin solution film (< 0.1 mm) between the gas layer and the wall of the FEP tubing. It was shown that more effective photoirradiation derived from the short path length could be achieved in this area [8]. Similarly, Oelgemöller's group

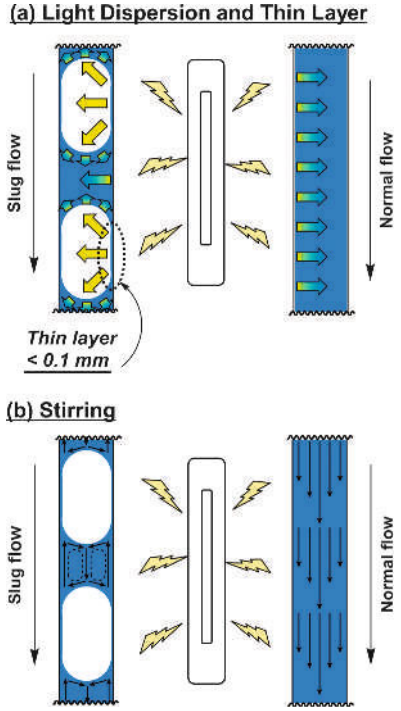

Figure 3. Effects on photoirradiation of the slug flow modes

Table 3. Reactor parameters for each condition

Parameter	Batch	Microcapillary reactor (method nos.1, 3)
Path length (mm)	14.0	1.0
Aperature (cm^2)	5.7[a]	52.4[b]
Irradiated area[c] (cm^2)	2.85	15.7
Irradiated volume (cm^3)	2.0	0.785
Irradiated area/volume ratio (m^2 m^{-3})	143	2000
Lamp power (W)	500	500
Lamp power/aperature (W cm^{-2})	87.6	9.54
Lamp power/irradiated area (W cm^{-2})	174.8	31.85

[a] Assuming cylindrical geometries. [b] Covered quartz immersion well area by microcapillary. [c] Assuming that only half of the tube/capillary is irradiated.

obtained thin solution films using O_2 gas as a reagent for a photoreaction [9], and Zhang's group reported that a thin liquid film was constructed by slug flow conditions using MeOH and oil and could be applied to synthesize biodiesel [16]. These reports suggest that, in the present study, a third reason for the enhanced performance may be that a thin solution layer could be forming between the inactive reagent and the FEP tube wall. In this area, a short path length could be achieved, thereby improving the photoirradiation. The combination of these three factors resulted in a greatly enhanced photoreaction under slug flow conditions.

The important reactor parameters of these irradiation conditions are listed in Table 3. The irradiated area to volume ratio in all conditions using capillary reactor was 2000 m^2 m^{-3}, which was almost 14 times larger than that of the batch reactor, 143 m^2 m^{-3}. The calculated lamp power to irradiated area (W cm^{-2}) in the batch reactor was significantly higher than that of capillary reactor. On the other hand, the irradiation time to complete the photoreaction in the capillary reactor was shorter than that of Pyrex test tube. The result indicates that the microcapillary module wrapped around immersion well could cover the emissive area of the lamp more effectively than the batch reactor.

From the parameters of the reactor, the energy efficiencies of each of the conditions were calculated (Table 4). The simple capillary reactor with normal flow gave a higher energy efficiency (%W^{-1} h^{-1}) than that of the Pyrex test tube; whereas, there was no great difference in energy efficiency per irradiated area (%W^{-1} h^{-1} cm^{-2}) between these two conditions. On the other hand, with the slug flow using the substrate solution and H_2O in the microcapillary, all the obtained values were significantly higher than those for both the normal flow and batch conditions. From these data, the slug flow method utilizing the inactive reagent was demonstrated to dramatically improve the efficiency of the photoreaction.

3. Conclusion

We constructed a simple microcapillary reactor using FEP capillary tubing and applied it to an asymmetric Paternò–Büchi-type photoreaction. While the microcapillary reactor could not enhance the diastereoselectivity, the photoreaction efficiency was dramatically improved compared to the use of a conventional batch reactor. In addition, we demonstrated that the slug flow conditions using the reaction solution and H_2O in the microcapillary system resulted in greater efficiency than that achieved using normal one-layer flow. This was attributed to

Table 4. Energy efficiencies

Reactor	Yield (%)	Irr. time (sec)	Energy efficiencies	
			%W^{-1} h^{-1}	%W^{-1} h^{-1} cm^{-2}
Batch	40	180	1.60	0.561
Method no.1	39	30	9.36	0.596
Method no.3	45	15	21.6	1.376

three factors: a light dispersion effect, a stirring effect, and a thin layer film effect. These results clearly demonstrated the potential of this irradiation method for use in photoreactions.

4. Experimental

4.1. General. Benzoylformic acid, *l*-menthol, 4-dimethylaminopyridine (DMAP), *N,N'*-diisopropylcarbodiimide (DIPC) and *n*-tetracosane (analytical standard grade) was purchased and used without further purification. Dichloromethane (DCM) was purchased as a dry solvent and used without further purification. Toluene was purchased as a spectrograde solvent, and used without further purification. 2,3-Dimethyl-2-butene **2** was used after distillation. All reactions and manipulations of air- and moisture-sensitive compounds were carried out under an atmosphere of dry N_2 using standard vacuum line techniques. Melting points were determined using B-545 melting point apparatus. Optical rotations were determined on a DIP-1000 digital polarimeter using the sodium D line. Infrared (IR) spectra were obtained on a FT/IR-4200. High-resolution mass spectra (HRMS) were obtained on a JMS-700 instrument. Flash column chromatography was performed with silica gel 60 N. ^{1}H NMR and ^{13}C NMR spectra were obtained on a JNM-ECP500NK. NMR date are reported as chemical shift in ppm (δ), integration, multiplicity (s=singlet, d=doublet, t=triplet, q=quartet, td=triplet of doublet, brs=broad singlet, m=multiplet), and coupling constant (*J* in Hz). ^{1}H NMR spectra are reported using TMS as internal standard (δ=0.0 ppm). ^{13}C NMR spectra are reported based on the middle peak of $CDCl_3$ as internal standard (δ=77.0 ppm). X-ray crystallographic analysis: measurements were carried out on a RAXIS-RAPID diffractometer using filtered Mo-Kα radiation at −150 °C.

4.2. Synthesis of Substrate 1. Benzoylformic acid (1.50 g, 10.0 mmol), *l*-menthol (1.56 g, 10.0 mmol), and DMAP (610.1 mg, 0.50 mmol) were dissolved in DCM (100 mL). The reaction mixture was cooled to 0 °C and then stirred for 10 min. DIPC (1.86 mL, 12.0 mmol) was added dropwise to the solution, and the reaction mixture was stirred at 0 °C for 30 min, and then overnight at rt (Room temperature). The reaction was quenched by the addition of 2 N HCl aq. The crude solution was then extracted with DCM, and the organic layer was washed by brine and dried over $MgSO_4$. The reaction mixture was purified using silica gel column chromatography (*n*-hexane/AcOEt=97:3). After recrystallization from *n*-hexane, product **1** was obtained as a colorless solid (1.76 g, 61.0%).

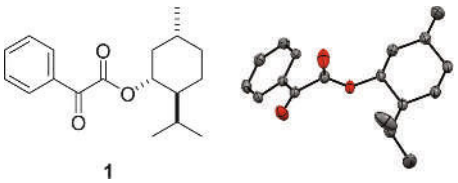

1

mp=72 °C (*n*-hexane); $[\alpha]_D^{27}$=−0.63 (c=1.0 in MeOH); ^{1}H NMR ($CDCl_3$) δ: 7.98 (2H, m), 7.66 (1H, m), 7.53 (2H, m), 5.01 (1H, td, *J*=10.8, 4.8 Hz), 2.20–2.16 (1H, m), 2.00–1.91 (1H, m), 1.76–1.72 (2H, m), 1.61–1.49 (2H, m), 1.23–1.08 (2H, m), 0.96 (3H, d, *J*=7.0 Hz), 0.94–0.89 (4H, m), 0.85 (3H, d, *J*=7.0 Hz); ^{13}C NMR ($CDCl_3$) δ: 186.83, 163.89, 134.81, 132.49, 129.90, 128.89, 46.75, 40.58, 34.01, 31.52, 26.10, 23.26, 21.95, 20.67, 16.11; IR (KBr) 2957, 2877, 1735, 1685 cm^{-1}; HRMS (ESI+) Calcd for $C_{18}H_{24}O_3Na$ $(M+Na)^+$ 311.1623, found 311.1623.

X-ray crystallographic analysis:

$C_{18}H_{24}O_3$; colorless block; (0.150×0.040×0.040 mm); orthorhombic; space group=$P2_12_12_1$(#19); Z=4; *a*=8.1656(2) Å, *b*=12.0492(3) Å, *c*=16.7765(4) Å, *V*=1650.63(6) Å^3; ρ calcd=1.160 g/cm^3. The structure was solved using direct methods and refined with a full matrix against all F^2 data. Hydrogen atoms were calculated in riding positions. *wR*2=0.1038 and *R*=0.0589.

4.3. Photoreactions under Each Set of Conditions, and Product Analysis

4.3.1. Apparatus for Photoreactions. For all conditions, a HALOS 500 W high-pressure Hg lamp was employed as the light source, with a quartz immersion well (o.d.: 17.5 cm), and the reaction setup was placed in a MeOH-containing cooling bath. For the flow conditions, the FEP tubing (i.d.: 1.0 mm; λ> 230 nm) was used as an irradiation unit and was tightly wrapped around a quartz immersion well. The solutions of substrates **1** and **2**, and the H_2O flow rates, were controlled using a programmable syringe pump (YMC Co., Ltd., YSP-101). When N_2 gas was used, the gas flow rate was controlled using a mass flow controller (KOFLOC, Model8500M-0-1-1). A μ-mixer (MiChS, i.d.; 200 μm) was employed as a T-shaped connector.

4.3.2. Photoreaction in a Pyrex Test Tube (Batch Condition). Substrate **1** (28.4 mg, 0.1 mmol) and *n*-tetracosane (6.8 mg, 0.02 mmol) were dissolved in toluene (2.0 mL) in a Pyrex test tube (i.d.: 14.0 mm; λ >280 nm), and the solution was purged with N_2 for 10 min at 0 °C. 2,3-Dimethyl-2-butene **2** (21.8 μL, 0.2 mmol) was then added to the solution. A balloon containing N_2 was attached to the top of the test tube and the irradiation was carried out at 10 °C within MeOH cooling bath. After a set irradiation period, the solvent was carefully evaporated. The product was purified using silica gel column chromatography, and diastereomers **3**, **4** were obtained as single isomers. The diastereomeric excess (d.e.) values and yields were subsequently determined using GC, with *n*-tetracosane as internal standard.

4.3.3. Photoreaction in a Capillary Reactor under Normal Flow Conditions (Method No. 1). A 1.0 m FEP tube was wrapped around the quartz immersion well in six windings. A solution of substrate **1** (72.1 mg, 0.25 mmol), *n*-tetracosane (16.9 mg, 0.05 mmol), and 2,3-dimethyl-2-butene **2** (54.6 μL, 0.5 mmol) in toluene (5.0 mL) was loaded into a gas-tight syringe, and attached to a syringe pump. The solution flow rate was adjusted according to the target irradiation time, i.e., exposure to light in the capillary. The irradiation unit was maintained at 10 °C throughput. After irradiation, the d.e. values and yields were determined using GC, with *n*-tetracosane as internal standard.

4.3.4. Photoreaction in a Capillary Reactor under Slug Flow Conditions Using N_2 Gas (Method No. 2). A 5.0 m FEP tube was wrapped around the quartz immersion well in 30 windings. A solution of substrate **1** (72.1 mg, 0.25 mmol), *n*-tetracosane (16.9 mg, 0.05 mmol), and 2,3-dimethyl-2-butene **2** (54.6 μL, 0.5 mmol) in toluene (5.0 mL) was loaded into a gas-tight syringe attached to a syringe pump. N_2 gas was provided by a cylinder attached to a mass flow controller. T-shaped mixer inlets were connected to the N_2 flow controller and solution gas-tight syringe, and the outlet was connected to the irradiation unit. The irradiation unit was maintained at 10 °C, and the gas and solution flow rates were adjusted to create a stable slug flow pattern. After stable reaction conditions were achieved, 1.0 mL of the solution was collected for analysis. After irradiation, the d.e. values and yields were determined using GC, with *n*-tetracosane as internal standard.

4.3.5. Photoreaction in a Capillary Reactor under Slug Flow Condition with H_2O (Method No. 3). A 1.0 m FEP tube was wrapped around the quartz immersion well in 6 windings. A solution of substrate **1** (72.1 mg, 0.25 mmol), *n*-tetracosane (16.9 mg, 0.05 mmol) and 2,3-dimethyl-2-butene **2** (54.6 μL, 0.5 mmol) in toluene (5.0 mL), and H_2O (5.0 mL) were separately loaded into gas-tight syringes attached to a syringe pump.

T-shaped mixer inlets were connected to both gas-tight syringes, and the outlet was connected to the irradiation unit. The substrate solution and H_2O flow rates were adjusted according to the irradiation time. The irradiation unit was maintained at 10 °C. After irradiation, the d.e. values and yields were determined using GC, with *n*-tetracosane as internal standard.

4.3.6. Product Analysis. Analytical GC was carried out using a G-3500 with a ZB-WAXplus column. The column oven temperature was maintained at 180 °C and the injection and detector were maintained at 230 °C. The peak corresponding to substrate **1** overlapped with a peak resulting from a by-product, making it difficult to calculate the conversion rate of **1** using this particular analysis method. Therefore, the conversion rate was determined using ^{1}H NMR analysis.

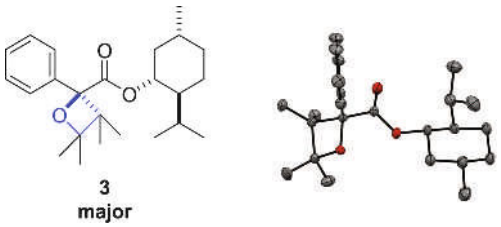

Major Product ***3***. Colorless solid; mp=80 °C (*n*-hexane); $[\alpha]_D^{28}$=−0.62 (c=1.0 in MeOH); ^{1}H NMR ($CDCl_3$) δ: 7.59−7.57 (2H, m), 7.31 (2H, dd, *J*=7.8, 7.8 Hz), 7.27−7.24 (1H, m), 4.72 (1H, td, *J*=10.8, 4.7 Hz), 1.95−1.91 (1H, m), 1.66−1.57 (2H, m), 1.50−1.40 (6H, m), 1.35 (3H, s), 1.26 (3H, s), 1.13−1.06 (1H, m), 0.99−0.80 (8H, m), 0.65 (3H, d, *J*=7.0 Hz), 0.34 (3H, d, *J*=7.0 Hz); ^{13}C NMR ($CDCl_3$) δ: 172.58, 139.53, 127.52, 127.28, 125.79, 88.35, 84.97, 75.05, 46.99, 46.72, 40.60, 34.14, 31.48, 25.53, 25.51, 25.31, 22.97, 22.47, 22.01, 20.51, 15.40; IR (KBr) 2996, 2957, 2930, 2866, 1715 cm^{-1}; HRMS (ESI+) Calcd for $C_{24}H_{36}O_3Na$ $(M+Na)^+$ 395.2562, found 395.2559.

X-ray crystallographic analysis:

$C_{24}H_{36}O_3$; colorless block; (0.12×0.11×0.10 mm); orthorhombic; space group=$P2_12_12_1$(#19); Z=4; *a*=6.3861(2) Å, *b*=17.4478(4) Å, *c*=19.8843(8) Å, *V*=2215.55(8) Å^3; ρ calcd=1.117 g/cm^3. The structure was solved by direct methods and refined with full matrix against all F^2 data. Hydrogen atoms were calculated in riding positions. *wR*2=0.0859 and *R*=0.0344.

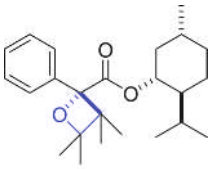

Minor Product ***4***. Colorless oil; $[\alpha]_D^{28}$=−0.41 (c=0.18 in MeOH); ^{1}H NMR ($CDCl_3$) δ: 7.62−7.60 (2H, m), 7.32 (2H, dd, *J*=7.8, 7.8 Hz), 7.28−7.25 (1H, m), 4.77 (1H, td, *J*=10.9, 4.7 Hz), 1.84−1.80 (1H, m), 1.72−1.62 (3H, m), 1.48−1.21 (11H, m), 1.04−0.78 (12H, m), 0.64 (3H, d, *J*=6.5 Hz); ^{13}C NMR ($CDCl_3$) δ: 172.25, 139.51, 126.19, 88.44, 84.90, 75.06, 46.78, 46.76, 40.43, 34.12, 31.40, 25.74, 25.49, 22.79, 22.67, 22.26, 21.95, 20.78, 15.45; IR (neat) 2956, 2926, 2870, 1740, 1718 cm^{-1}; HRMS (ESI+) Calcd for $C_{24}H_{36}O_3Na$ $(M+Na)^+$ 395.25652, found 395.2564

CCDC-965325 (major product **3**) and CCDC-965326 (substrate **1**) contain the supplementary crystallographic data for this paper. These data can be obtained free of charge from The Cambridge Crystallographic Data Centre via http://www.ccdc.cam.ac.uk/products/csd/request/.

Acknowledgments. We thank Ms. Y. Nishikawa for conducting the HRMS measurements and Mr. S. Katao for the X-ray crystal analysis. This work was supported in part by a Grant-in Aid for Scientific Research on Innovative Areas Grant no. 24106629 and the Scientific Research (B) nos. 21310081 and 24310101. K.T. thanks JSPS Fellows Grant no. 9185 from the Ministry of Education, Culture, Sports, Science and Technology (MEXT) of the Japanese Government and by the Foundation of the Nara Institute of Science and Technology.

References

1. (a) Ciana, C.-L.; Bochet C. G. *Chimia* **2007**, *61*, 650; (b) Oelgemöller, M.; Healy, N.; de Oliveira, L.; Jung, C.; Mattay J. *Green Chem.* **2006**, *8*, 831; (c) Hoffmann, N. *Chem. Rev.* **2008**, *108,* 1052; (d) Bach, T.; Hehn, J. P. *Angew. Chem. Int. Ed.* **2011**, *50*, 1000.

2. For reviews and important reports on microreactors; (a) Yoshida, J. *Flash Chemistry: Fast Organic Synthesis in Microsystems*; Wiley: Hoboken, 2008; (b) Fukuyama, T.; Rahman, M. T.; Sato, M.; Ryu, I.; *Synlett* **2008**, 151; (c) Yoshida, J.; Nagaki, A.; Yamada, T. *Chem. –Eur. J.* **2008**, *14*, 7450; (d) McMullen, J. P.; Jensen, K. F. *Annu. Rev. Anal. Chem.* **2010**, *3*, 19; (e) Razzaq, T.; Kappe, C. O. *Chem. –Asian J.* **2010**, *5*, 1274; (f) Suga, S.; Yamada, D.; Yoshida, J. *Chem. Lett.* **2010**, *39*, 404; (g) Yoshida, J.; Kim, H.; Nagaki, A. *ChemSusChem* **2011**, *4*, 331; (h) Pastre, J. C.; Browne, D. L.; Ley, S. V. *Chem. Soc. Rev.* **2013**, *42*, 8849.

3. For reviews on photoreaction using microreactors; (a) Matsushita, Y.; Ichimura, T.; Ohba, N.; Kumada, S.; Sakeda, K. Suzuki, T.; Tanibata, H.; Murata, T. *Pure Appl. Chem.* **2007**, *79*, 1959; (b) Knowles. J. P.; Elliott, L. D.; Booker-Milburn, K. I. *Beilstein J. Org. Chem.* **2012**, *8*, 2025; (c) Shvydkiv, O.; Oelgemöller, M. *CRC handbook of Organic Photochemistry and Photobiology*; Griesbeck, A.; Oelgemöller, M.; Ghetti, F., Ed.; CRC Press: Boca Raton, 2012, pp. 49–72; (d) Noël, T.; Wang, X.; Hessel, V. *Chimia Oggi* **2013**, *31*, 10.

4. (a) Asano, K.; Uesugi, Y.; Yoshida, J. *Org. Lett.* **2013**, *15*, 2398; (b) Lumley, E. K.; Dyer, C. E.; Pamme, N.; Boyle, R. W. *Org. Lett.* **2012**, *14*, 5724; (c) Fukuyama, T.; Kajihara, Y.; Hino, Y.; Ryu, I. *J. Flow Chem.* **2011**, *1*, 40; (d) Fuse, S.; Mifune, Y.; Tanabe, N.; Takahashi, T. *Org. Biomol. Chem.* **2012**, *10*, 5205; (e) Kopetzki, D.; Levesque, F.; Seeberger, P. H. *Chem. – Eur. J.* **2013**, *19*, 5450.

5. For recent examples of photoreactions using microreactors; (a) Mukae, H.; Maeda, H.; Nashihara, S.; Mizuno, K. *Bull. Chem. Soc. Jpn.* **2007**, *80*, 1157; (b) Horie, T.; Sumino, M.; Tanaka, T.; Matsushita, Y.; Ichimura, T.; Yoshida, J. *Org. Proc. Res. Dev.* **2010**, *14*, 405; (c) Yavorskyy, A.; Shvydkiv, O.; Hoffmann, N.; Nolan, K.; Oelgemöller, M. *Org. Lett.* **2012**, *14*, 4342; (d) Maskill, K. G.; Knowles, J. P.; Elliott, L. D.; Alder, R. W.; Booker-Milburn, K. I. *Angew. Chem. Int. Ed.* **2013**, *52*, 1499; (e) Claudius-Brandt, S.; Kupracz, L.; Kirshning, A. *Beilstein J. Org. Chem.* **2013**, *9*, 1745; (f) Wojcik, F.; O`Brien, A. G.; Gotze, S.; Seeberger, P. H.; Hartmann, L. *Chem. – Eur. J.* **2013**, *19*, 3090.

6. (a) Maeda, H.; Mukae, H.; Mizuno, K. *Chem. Lett.* **2005**, *34*, 66; (b) Sakeda, K.; Wakabayashi, K.; Matsushita, Y.; Ichimura, T.; Suzuki, T.; Wada, T.; Inoue, Y. *J. Photochem. Photobiol. A: Chem.* **2007**, *192*, 166.

7. (a) Tsutsumi, K.; Terao, K.; Yamaguchi, H.; Yoshimura, S.; Morimoto, T.; Kakiuchi, K.; Fukuyama, T.; Ryu, I. *Chem. Lett.* **2010**, *16*, 7448; (b) Terao. K.; Nishiyama, Y.; Aida, S.; Tanimoto, H.; Morimoto, T.; Kakiuchi. K. *J. Photochem. Photobiol. A: Chem.* **2012**, *242*, 13.

8. Terao, K.; Nishiyama, Y.; Tanimoto, H.; Morimoto, T.; Oelgemöller, M.; Kakiuchi, K. *J. Flow Chem.* **2012**, *2*, 73.

9. Yavorskyy, A.; Shvydkiv, O.; Limburq, C.; Nolan, K.; Delaure, Y. M. C.; Oelgemöller, M. *Green Chem.* **2012**, *14*, 888.

10. Gotthardt, H.; Lenz, W. *Angew. Chem. Int. Ed.* **1979**, *18*, 868.

11. (a) Bach, T. *Synthesis* **1998**, 683; (b) D`Auria, M.; Racioppi, R. *Molecules* **2013**, *18*, 11384.

12. Shen, B.; Jamison, T. F. *Aust. J. Chem.* **2013**, *66*, 157.

13. From the catalogue, Seishin Enterprise Co., Ltd.. http://www.betterseishin.co.jp/download/pdf/kussetu.pdf

14. From the catalogue, Wako Pure Chemical Industries Ltd.. http://www.siyaku.com/uh/Shs.do?dspCode=W01W0120-0187

15. (a) Burns, J. R.; Ramshaw, C. *Lab Chip* **2001**, *1*, 10; (b) Fries, D. M.; Waelchli, S.; Rudolf von Rohr, P. *Chem. Eng. J.* **2008**, *135S*, S37.

16 Su, J.; Ju, J.; Ji, L.; Zhang, L.; Xu, N. *Ind. Eng. Chem. Res.* **2008**, *47*, 1398.